NANO LETTERS

2006
Vol. 6, No. 7
1415−1419

The Nature of Contact between Pd Leads and Semiconducting Carbon Nanotubes

Wenguang Zhu[†,‡] and Efthimios Kaxiras*[,†]

Department of Physics and Division of Engineering and Applied Sciences, Harvard University, Cambridge, Massachusetts 02138, and Center for Computational Materials, Institute for Computational Engineering and Sciences, Departments of Physics and Chemical Engineering, University of Texas, Austin, Texas 78712

Received February 23, 2006; Revised Manuscript Received May 5, 2006

ABSTRACT

The contact between semiconducting single-wall carbon nanotubes (SWCNTs) and metallic leads is of central importance to potential electronic device applications. We investigate the nature of the contact of SWCNTs with Pd leads in a fully covered geometry that closely resembles experimental setups. We employ first-principles calculations within density functional theory to obtain the equilibrium structure for representative semiconducting SWCNTs embedded in Pd and analyze their electronic structure features, charge-transfer effects, electrostatic potentials, and Fermi level alignment at the interfaces with the metal contact. We find that there is no electrostatic or Schottky-type barrier to electron transfer between the metal and the nanotube.

Nanostructures provide unique opportunities for vastly improving the performance of electronic devices through the realization of molecular computing, based on components with ultrahigh density of elements and speed of operation.[1] Among the various possible nanoscale elements for molecular devices, carbon nanotubes (CNTs) have emerged as one of the most promising building blocks because of their size, structural strength, and extraordinary electronic properties.[2,3] Since they were first synthesized,[4] these intriguing carbon structures have received extensive attention.[5] Recently, it has been demonstrated[6−11] that an individual semiconducting CNT can operate either as a conventional MOSFET[12] or an unconventional Schottky barrier transistor[13] when it forms a contact with a metal electrode, with the type of behavior depending on the properties of the metal/CNT contact. The interaction between the carbon nanotube and the metal leads, and the resulting electronic structure effects, are crucial for the performance of the carbon nanotube field-effect transistor (CNFET).[13,14]

Theoretical studies have addressed certain aspects of the structure and electronic properties of model systems involving metal contacts and semiconducting CNTs.[15−17] From such studies, the Schottky barrier and tunneling barrier height were determined as a function of the atomic geometry,[16] and electronic charge transfer between the CNT and the metal contact was shown to depend on the electronic structure of the adsorbed nanotube and the work function of the metal surfaces.[17] In these studies, the metal/CNT contacts are modeled by simply having the nanotubes adsorbed on flat metal surfaces or placing them between two parallel metal surfaces.[15−17] Recent experimental studies have shown that the variation in nanotube diameter is largely responsible for the performance of a CNFET,[18,19] with the best performance achieved by combining Pd contacts with CNTs of diameters larger than 1.4 nm.[18] In the experimental studies, a section of the nanotube is fully embedded in the metal lead and the details of the interface geometry are believed to affect strongly the nature of the contact.

In this paper, we use first-principles calculations to study the electronic structure of the contact between semiconducting single-wall carbon nanotubes (SWCNTs) and Pd metal leads, in a fully covered geometry that resembles closely the experimental setups.[18,19] We considered two representative semiconducting SWCNTs, the zigzag (8,0) and (10,0) structures. These structures embedded in several layers of the metal contact, represent systems close to the limit of what can be handled by existing computational resources (see details below). Moreover, the variation of electronic transport properties is more pronounced for small diameter nanotubes, so these choices are useful in establishing the limit of expected behavior. We find that for both the (8,0) and (10,0) SWCNTs the surrounding metal lead can induce a significant deformation on the nanotube when the combined structure is allowed attain its optimal structure. The calculated electrostatic potential reveals that there exists no barrier, at least in the channels relevant to electron transport, at the

[†] Harvard University.
[‡] University of Texas.

10.1021/nl0604311 CCC: $33.50
Published on Web 06/17/2006

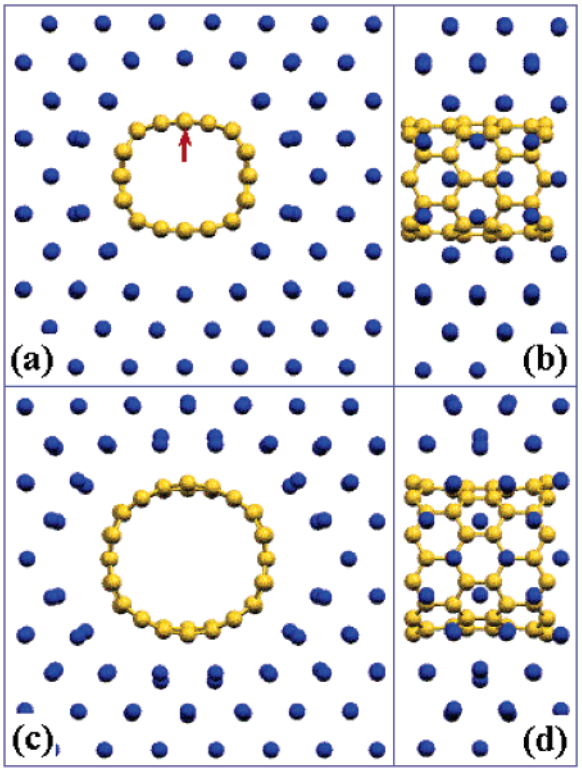

Figure 1. Atomic structure of the Pd/CNT system, including full relaxation: In (a) and (b) we show two views of the (8,0) nanotube fully covered by Pd, (a) along and (b) perpendicular to the nanotube axis; (c) and (d) are the corresponding views of the (10,0) Pd-covered CNT. The red arrow in (a) indicates the C atom we chose as a reference for lining up the energy levels in the density of states plots (Figure 4).

interface of the nanotubes and the metal contact. Using charge difference distributions, we find that electrons are transferred from the nanotube as well as from the surrounding metal Pd to the interface region. Finally, the electronic densities of states indicate clearly that interface states induced by the Pd/CNT contact fill the band gap of the semiconducting CNT, resulting in a contact of metallic nature.

Our first-principles calculations are based on density functional theory and the Perdew−Wang 1991 version of the generalized gradient approximation (PW91-GGA),[20] as implemented in VASP.[21] Default plane-wave cutoffs from the GGA ultrasoft-pseudopotential database[22] are used for both Pd and C in the calculations. The Monkhorst−Pack scheme[23] is employed for Brillouin zone sampling. Optimized atomic geometries are achieved when the magnitude of the forces on all unconstrained atoms is smaller than 0.03 eV/Å. These choices of computational parameters produce a lattice constant of 3.962 Å for bulk face-centered cubic (fcc) Pd, compared to the experimental value of 3.890 Å; the calculated diameters of the free-standing (8,0) and (10,0) SWCNTs are 6.37 and 7.90 Å.

To model an infinite carbon nanotube fully covered by Pd, we start with a perfect Pd fcc crystal and remove just enough Pd atoms for the nanotube to fit into the opening. The constructed supercells are shown in Figure 1 for the (8,0) and (10,0) SWCNTs, respectively. The direction of the nanotube axis is parallel to the ⟨110⟩ direction of the Pd crystal. In this direction, three periods of Pd crystal (2.80 Å × 3) match very well with two periods of the zigzag (8,0) and (10,0) nanotube (4.26 Å × 2), with a difference in lattice parameter between the two superstructures of only 1.4%. A sufficient amount of Pd layers must be included to ensure that it represents well the bulk metal limit away from the interface. The resulting supercell size is 19.8 Å × 19.6 Å × 8.4 Å, and contains 64 C atoms and 168 Pd atoms for the (8,0) nanotube and 80 C atoms and 153 Pd atoms for the (10,0) nanotube. The size of the holes in the metal is chosen as small as possible to accommodate the nanotube, the only requirement being that the combined systems have a net energy gain relative to the isolated components. This requirement ensures that the model contact does not involve unphysical configurations with atoms on either side that are too close to each other. The cross section of the holes in the Pd lead is hexagonal, with the inner surfaces consisting of the close-packed Pd(111) and (100) facets. Figure 1 shows the optimized structures, in which both SWCNTs are deformed in the radial direction. The shortest distances between C and Pd atoms are 2.24 Å and 2.22 Å for the (8,0) and (10,0) nanotubes, respectively. Our extensive calculations for both systems show that the basic properties of the contacts are qualitatively very similar. Accordingly, we will focus our attention to the Pd-covered (8,0) nanotube.

The calculated self-consistent-field electrostatic potential of the Pd covered (8,0) SWNT is presented in Figure 2. Figure 2a is a contour plot of the electrostatic potential in the plane perpendicular to the nanotube axis, indicated by the red line as shown in the inset. Other cross sections, such as one indicated by the blue line in the same inset, exhibit very similar features in the electrostatic potential as Figure 2a. Blue and red areas in these contour plots represent regions where the electrostatic potential is lower and higher than the Fermi level of the system, respectively. The other two representative contour plots of electrostatic potential, shown in parts b and c of Figure 2, correspond to cross sections passing through the planes on which the carbon atoms of the nanotube are in the closest contact with surrounding Pd atoms; these cross sections are indicated in the inset of Figure 2d as dashed red lines, with the corresonding labels (b) and (c). The existence of contiguous blue areas extending from the nanotube to the metal Pd through the interface indicates that the electron from the nanotube can be ballistically transferred to the metal electrode without any electrostatic potential barrier. A more quantitative analysis of the same features is shown in Figure 2d, in which we plot the variation of electrostatic potential along the direction of five lines passing through C and Pd atoms. The colors of the curves in this figure correspond to the colors of the dashed lines shown in parts b and c of Figure 2, which connect C atoms on the nanotube to their close Pd neighbors in the metal. The Fermi level is shifted to zero and denoted by a red dotted line. The line scans extend from the center of the tube ($x = -3$ Å) to well within the metal ($x = +3$ Å). As is clearly seen from this plot, the electrostatic potential is always lower than the Fermi level, by about ∼3 eV at its highest value, along several paths from a C atom to a close neighbor Pd

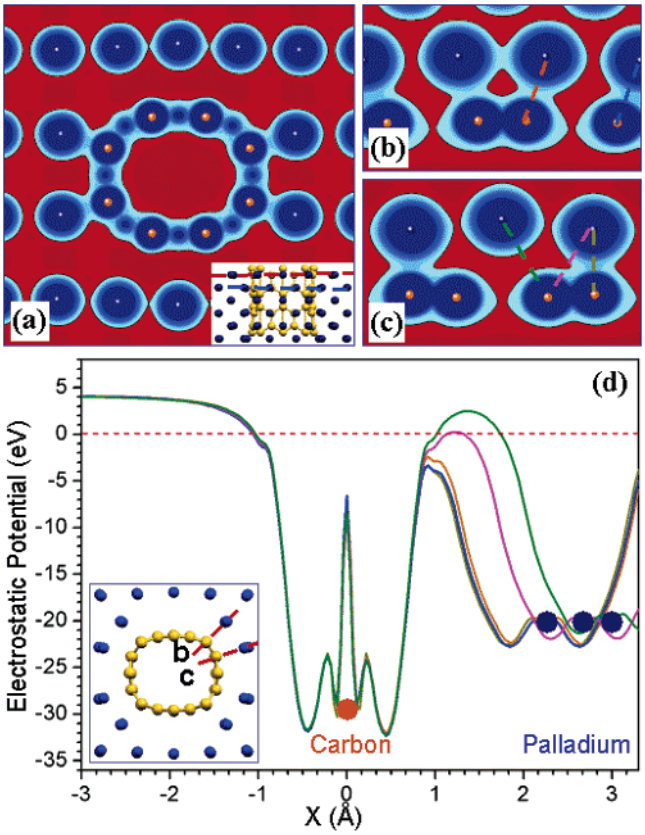

Figure 2. The calculated self-consistent electrostatic potential for the Pd-covered (8,0) nanotube: (a) contours of constant potential plotted in a cross section, indicated by the red line in the inset. In (b) and (c) the potential contours on two different cross sections are shown, which are indicated by red lines in the inset of (d), with corresponding labels. In these plots, blue represents negative values and red positive values of the electrostatic potential, relative to the Fermi level. In (d), we show the electrostatic potential along five directions passing through C and Pd atoms near the contact region, and extending from the center of the nanotube ($x = -3$ Å) to well within the metal region ($x = +3$ Å); the colors of the curves correspond to the colors of the dashed lines indicating those directions in panels b and c; the red dashed line indicates the Fermi level. In all panels C atoms are shown in orange and Pd atoms in blue; the positions of C atoms are set to zero in (d).

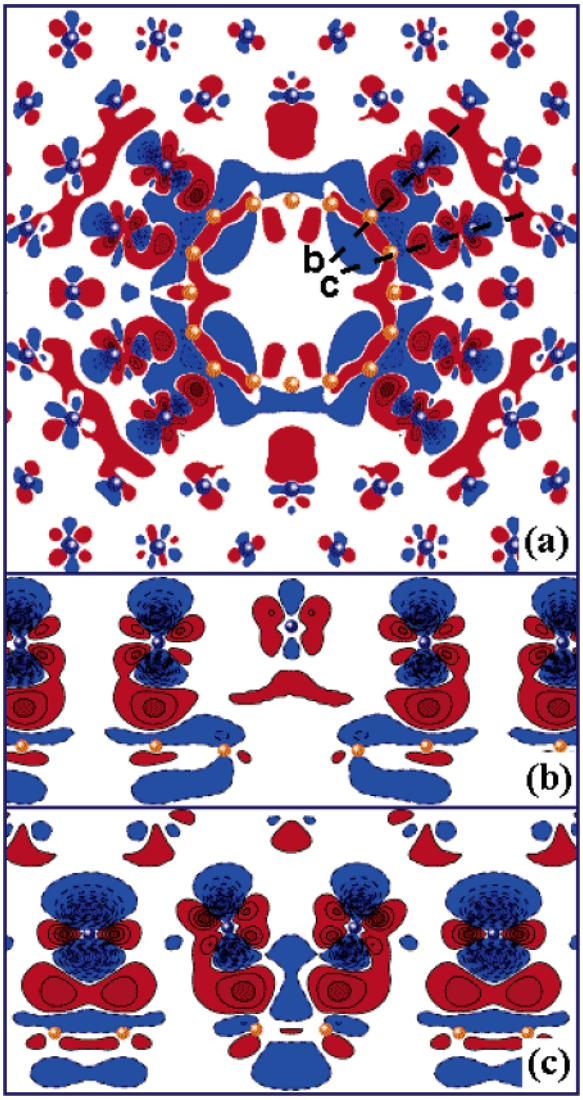

Figure 3. Charge density difference plots for the Pd-covered (8,0) nanotube: (a) integrated along the direction of the nanotube axis; (b) and (c) on the two cross sections indicated in (a) as black dashed lines. Red indicates accumulation of electronic charge density and blue depletion of electronic charge density. The positions of C and Pd atoms are denoted by symbols as in Figure 2.

atom (the orange, brown, and blue line scans), consistent with previous calculations on (8,0) SWCNT adsorbed on Pd(111) and (100) surfaces.[16] The electrostatic potential becomes higher than the Fermi level, indicating a barrier to the motion of electrons, only along directions in which there is a clear disruption of the contiguous blue regions, as, for example, along the pink and green line scans. Since there are several directions along which no barrier exists, we conclude that there is no electrostatic barrier to electron transport from the nanotube to the metal region.

We next perform an analysis of charge transfer between the (8,0) SWCNT and the metal Pd contact. Figure 3 shows the difference between the total charge density of the combined Pd/CNT system and the sum of the total charge density of the isolated nanotube and pure metal Pd, the latter two having exactly the same structure when considered separately as the structure they have in the combined system. In Figure 3a, the charge density difference, integrated in the direction parallel to the nanotube axis, is plotted on the plane perpendicular to the nanotube axis. The blue regions represent depletion of electrons while the red regions represent accumulation of electrons in the combined system relative to the two isolated components. In parts b and c of Figure 3 we show the same quantity on the two cross sections shown also in parts b and c of Figure 2. This set of results presents clear evidence that electrons leave from both components of the system near the interface and accumulate in the interface region, mostly between C and Pd close neighbors, which is similar to the case of a (10,0) nanotube absorbed on an Al(100) surface.[17] The depletion of electrons is most pronounced on the Pd atoms closest to the interface. It is interesting that, despite the higher electronegativity of C (2.5) relative to that of Pd (2.2), the electrons depleted from the Pd inner surface do not accumulate on the C sites but rather remain between the C and Pd atoms at the interface.

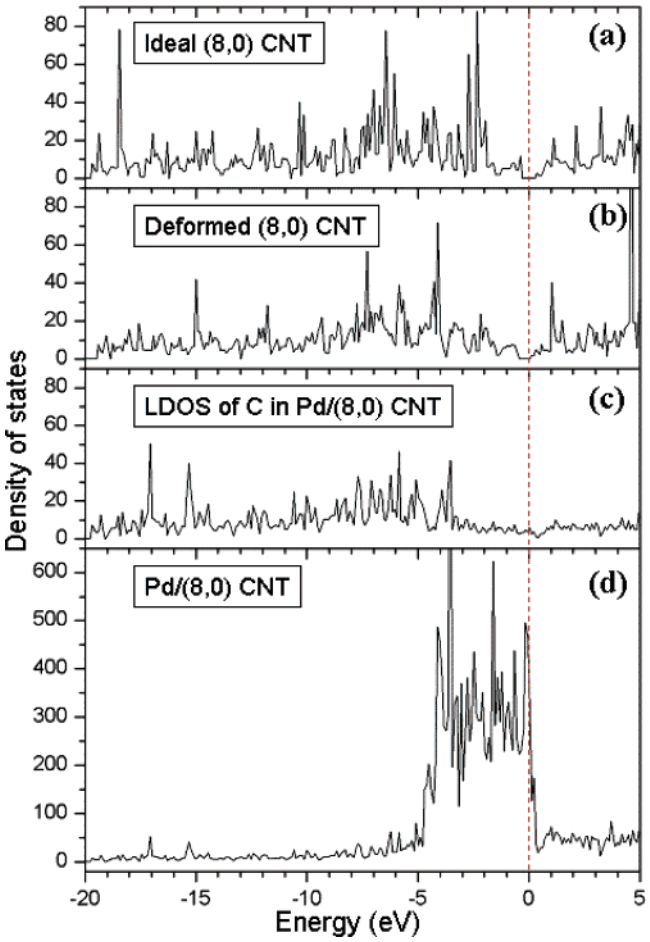

Figure 4. (a) DOS of a free-standing (8,0) CNT. (b) DOS of an isolated (8,0) CNT with the atomic structure of that embedded in Pd. (c) Projected DOS on C for the combined Pd/CNT system. (d) DOS of the combined Pd/CNT system. The vertical dotted red line denotes the Fermi level of the Pd/CNT system.

To illustrate the evolution of the electronic states from the free to the metal-covered nanotube, we plot in Figure 4 the density of states (DOS) for the free-standing (8,0) CNT (Figure 4a), the isolated nanotube deformed to the structure it assumes when in contact with Pd (Figure 4b), and the Pd/CNT combined system (Figure 4c). We align the energy levels of different calculations with the average potential at the atomic core of a C atom, denoted by the arrow in Figure 1a. Comparing the DOS of the free and deformed nanotubes, we find the deformation of the nanotube induces a narrowing of the band gap by 0.10 eV and a lowering of the valence band maximum by 0.14 eV. More importantly, in the Pd/CNT system, the site-projected DOS on the C atoms (Figure 4c) reveals that the band-gap region of the isolated nanotube is actually filled by interface states in the combined system. This indicates that when the nanotube is in contact with the Pd lead, there is no longer a semiconducting component in the system. The large density of states in the range within 5 eV below the Fermi level is due entirely to Pd d-states, which are nearly full. The position of the Fermi level is actually such that it requires some fraction of the Pd d-states to be partially filled, consistent with the partial depletion of electrons from the Pd side discussed in connection with the charge density difference.

As a final comment, we discuss how the results described above may be affected by the structural model we have adopted. In experiments, the contacts are formed by depositing the metal on the nanotube,[18] which might lead to structures different than those assumed here. However, such structures are likely to include even more close neighbors between the metal and the nanotube atoms, and it is these atomic arrangements that contribute to the barrierless transport of electrons across the interface. Interestingly, theoretical studies of SWCNTs covered by a single layer of metal atoms also exhibit the structural distortions observed in our model structures,[24] indicating that the electronic consequences of such distortions will also be present in experimentally accessible setups. Thus, we expect that the effects found by our study are likely to be enhanced in the experimental systems.

In summary, we studied the electronic structure of semiconducting SWCNTs fully covered by metal Pd contacts, in a geometry that is realistically close to experimental setups. We found that embedding the nanotube in a Pd metal contact has significant effects on the nanotube structure, which is distorted relative to its ideal structure in a vacuum. Moreover, we found that there is no electrostatic potential barrier for electron motion between the nanotube and the metal contact, as there are directions connecting C atoms to Pd close neighbors along which the potential is always below the Fermi level. We also found that electrons are depleted from both sides of the interface and accumulate in the regions between the two components of the system, with the depletion being more pronounced at Pd sites near the interface. Finally, the projected DOS indicates that in the combined Pd/CNT system there is no semiconducting component as a result of the existence of interface states whose energy lies within the SWCNT band gap.

Acknowledgment. We acknowledge useful discussions with Ph. Avouris. This work was sponsored by the Institute for the Theory of Advanced Materials in Information Technology (ITAMIT), University of Texas, Austin, which is funded by NSF Grant No. DMR-0325218.

References

(1) Rueckes, T.; Kim, K.; Joselevich, E.; Tseng, G. Y.; Cheung, C. L.; Lieber, C. M. *Science* **2000**, *289*, 94.
(2) Ouyang, M.; Huang, J. L.; Lieber, C. M. *Acc. Chem. Res.* **2002**, *35*, 1018.
(3) Ciraci, S.; Dag, S.; Yildirim, T.; Gülseren, O.; Senger, R. T. *J. Phys.: Condens. Matter* **2004**, *16*, R901.
(4) Iijima, S. *Nature* **1991**, *354*, 56.
(5) *Carbon Nanotubes*: *Synthesis, Structure, Properties, and Applications*; Dresselhaus, M. S., Dresselhaus, G., Avouris, Ph., Eds.; Springer-Verlag: Berlin, 2001.
(6) Tans, S. J.; Verschueren, A. R. M.; Dekker, C. *Nature* **1998**, *393*, 49.
(7) Bachtold, A.; Hadley, P.; Nakanishi, T.; Dekker, C. *Science* **2001**, *294*, 1317.
(8) Martel, R.; Schmidt, T.; Shea, H. R.; Hertel, T.; Avouris, Ph. *Appl. Phys. Lett.* **1998**, *73*, 2447.
(9) Martel, R.; Derycke, V.; Lavoie, C.; Appenzeller, J.; Chan, K. K.; Tersoff, J.; Avouris, Ph. *Phys. Rev. Lett.* **2001**, *87*, 256805.
(10) Javey, A.; Guo, J.; Wang, Q.; Lundstrom, M.; Dai, H. *Nature* **2003**, *424*, 654.

(11) Mann, D.; Javey, A.; Kong, J.; Wang, Q.; Dai, H. *Nano Lett.* **2003**, *3*, 1541.
(12) Heinze, S.; Radosavljević, M.; Tersoff, J.; Avouris, Ph. *Phys. Rev. B* **2003**, *68*, 235418.
(13) Heinze, S.; Tersoff, J.; Martel, R.; Derycke, V.; Appenzeller, J.; Avouris, Ph. *Phys. Rev. Lett.* **2002**, *89*, 106801.
(14) Léonard, F.; Tersoff, J. *Phys. Rev. Lett.* **2000**, *84*, 4693.
(15) Dag, S.; Gülseren, O.; Ciraci, S.; Yildirim, T. *Appl. Phys. Lett.* **2003**, *83*, 3180.
(16) Shan, B.; Cho, K. *Phys. Rev. B* **2004**, *70*, 233405.
(17) Okada, S.; Oshiyama, A. *Phys. Rev. Lett.* **2005**, *95*, 206804.
(18) Chen, Z.; Appenzeller, J.; Knoch, J.; Lin, Y.-M.; Avouris, Ph. *Nano Lett.* **2005**, *5*, 1497.
(19) Kim, W.; Javey, A.; Tu, R.; Cao, J.; Wang, Q.; Dai, H. *Appl. Phys. Lett.* **2005**, *87*, 173101.
(20) Perdew, J. P. In *Electronic Structure of Solids '91*; Ziesche, P., Eschrig, H., Eds.; Akademie: Berlin, 1991. Perdew, J. P.; Wang, Y. *Phys. Rev. B* **1992**, *45*, 13244.
(21) Kresse, G.; Furthmüller, J. *Phys. Rev. B* **1996**, *54*, 11169.
(22) Vanderbilt, D. *Phys. Rev. B* **1990**, *41*, 7892. Kresse, G.; Hafner, J. *J. Phys.: Condens. Matter* **1994**, *6*, 8245.
(23) Monkhorst, H. J.; Pack, J. D. *Phys. Rev. B* **1976**, *13*, 5188.
(24) Dag, S.; Durgun, E.; Ciraci, S. *Phys. Rev. B* **2004**, *69*, 121407.

NL0604311